Hindawi Publishing Corporation
International Journal of Analytical Chemistry
Volume 2014, Article ID 240197, 6 pages
http://dx.doi.org/10.1155/2014/240197

Research Article

Cyclic Nanostructures of Tungsten Oxide $(WO_3)_n$ $(n = 2–6)$ as NO_x Gas Sensor: A Theoretical Study

Mohammad Izadyar and Azam Jamsaz

Department of Chemistry, Faculty of Sciences, Ferdowsi University of Mashhad, 9177948974 Mashhad, Iran

Correspondence should be addressed to Mohammad Izadyar; izadyar@um.ac.ir

Received 30 August 2014; Accepted 8 November 2014; Published 2 December 2014

Academic Editor: Mohamed Abdel-Rehim

Today's WO_3-based gas sensors have received a lot of attention, because of important role as a sensitive layer for detection of the small quantities of NO_x. In this research, a theoretical study has been done on the sensing properties of different cyclic nanoclusters of $(WO_3)_n$ $(n = 2–6)$ for NO_x $(x = 1, 2)$ gases. Based on the calculated adsorption energies by B3LYP and X3LYP functionals, from the different orientations of NO_x molecule on the tungsten oxide clusters, O–N$\cdots$W was preferred. Different sizes of the mentioned clusters have been analyzed and W_2O_6 cluster was chosen as the best candidate for NO_x detection from the energy viewpoint. Using the concepts of the chemical hardness and electronic charge transfer, some correlations between the energy of adsorption and interaction energy have been established. These analyses confirmed that the adsorption energy will be boosted with charge transfer enhancement. However, the chemical hardness relationship is reversed. Finally, obtained results from the natural bond orbital and electronic density of states analysis confirmed the electronic charge transfer from the adsorbates to WO_3 clusters and Fermi level shifting after adsorption, respectively. The last parameter confirms that the cyclic clusters of tungsten oxide can be used as NO_x gas sensors.

1. Introduction

Semiconducting metal oxide sensors are one of the most studied groups of the chemical sensors which have been designed to react with gases [1]. Different materials such as SnO_2, WO_3, ZnO, MoO_3, TiO_2, InO_x, and mixed oxides have been studied and showed promising applications for detecting gases such as NO_x, O_3, NH_3, CO, CO_2, H_2S, and SO_x [2, 3]. Therefore, improvement in the sensitivity, selectivity, rate of gas response, and reliability of oxide semiconductor gas sensors is important [4–6].

Among various metal oxide semiconductors, tungsten oxide exhibits various special properties, which makes it very promising for applications in catalysis [7, 8] and detection of the toxic gases [9]. WO_3 based mixed oxides such as WO_3-Ti [10], WO_3-Pd, Pt, or Au [11], WO_3-In_2O_3 [12], and WO_3-Bi_2O_3 [13] have also been investigated for their sensing characteristics. These mixed oxides have been especially used in fabricating selective and sensitive NO_x gas sensors.

It was noted that different structures of WO_3 have excellent NO_x sensing layers [9]. This is because the W ions have different oxidation state (W^{6+}, W^{5+}) enhancing the adsorption activity of NO_x molecule on the surface of WO_3 structures [14, 15]. Recently, novel sensors based on tungsten oxide have been used for ozone monitoring [16, 17].

Tungsten oxide has attracted a lot of interests as an n-type oxide semiconductor [18]. WO_3 band gap has been measured by optical absorption in the range of 2.5 to 3.2 eV and is smaller than other semiconductors [19, 20]. For WO_3-based gas sensors, WO_3 plays a role as a sensitive layer for detecting small quantities of NO_x and such nanoscale assemblies can achieve high sensitivity and fast response times [21].

Despite the considerable amount of works done on WO_3 crystal structure so far, there are still important aspects of the electronic and structural properties of the WO_3 nanoclusters and NO_x adsorption which are unclear, especially for the small clusters of WO_3. Furthermore, the theoretical works which have been done so far are based on the standard DFT methods which seriously underestimate the semiconductor band gap. This problem can be improved by using DFT in combination with the hybrid functionals which provide

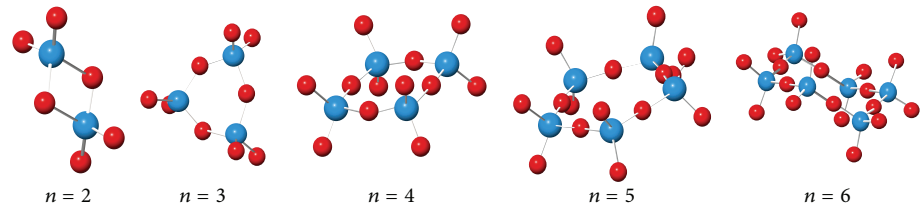

Figure 1: Optimized structures of the cyclic clusters of $(WO_3)_n$.

a satisfactory option for the description of both the electronic and the structural properties of WO_3 [22, 23].

In this work a theoretical procedure was applied to study the NO_x ($x = 1, 2$) adsorption on the $(WO_3)_n$ ($n = 2$–6) nanoclusters to evaluate the reactivity of WO_3 nanoclusters from the quantum chemistry point of view. Knowledge of the quantum reactivity indices and their role on the sensing properties of metal oxides is important to have an insight into the adsorption process and factors involved.

2. Computational Details

In order to study the NO_x ($x = 1, 2$) adsorption on the cyclic $(WO_3)_n$ ($n = 2$–6) nanoclusters, theoretically, DFT method has been applied. All the calculations have been carried out by using the GAUSSIAN 09 package [24]. LANL2DZ and 6-311++G(d,p) basis sets have been applied for W and other atoms, respectively [25–27]. $(WO_3)_n$ ($n = 2$–6) structures were generated in the vacuum and fully optimized using two kinds of hybrid functional of B3LYP and X3LYP. The adsorption of NO and NO_2 molecules on the clusters was investigated to evaluate some aspects of nanoclusters and NO_x interactions. Therefore, different orientations of NO_x on the nanoclusters were analyzed during these calculations. For geometry optimization, NO_x molecules were taken relaxed but the optimized structures of $(WO_3)_n$ ($n = 2$–6) were kept frozen. The adsorption energies of NO_x molecule and five different substrates have been computed according to

$$\Delta E = E\left[NO_x @ \left(WO_3\right)_n\right] - E\left(WO_3\right)_n - E\left(NO_x\right), \quad (1)$$

where $E[NO_x @ (WO_3)_n]$ is the total energy of the tungsten oxide cluster-NO_x complex and $E(WO_3)_n$ and $E(NO_x)$ are the total energy of the isolated $(WO_3)_n$ and NO_x, respectively.

Natural bond orbital (NBO) analysis which is suggested by Reed et al. [28, 29] was carried out to explore the distribution of the electrons into atomic and molecular orbitals. Based on these data, by HOMO-LUMO analysis, the stabilization energies were calculated. Chemical hardness, η, and charge transfer, ΔN, have been computed by Koopmans theorem [30], using the following, respectively:

$$\eta = \varepsilon_L - \varepsilon_H, \quad (2)$$

$$\Delta N = \frac{(\mu_B - \mu_A)}{(\eta_B + \eta_A)}, \quad (3)$$

$$\mu_e = \frac{(\varepsilon_L + \varepsilon_H)}{2}, \quad (4)$$

where ε_H and ε_L correspond to the Kohn and Sham [31] one-electron eigenvalues associated with the frontier molecular orbitals of HOMO and LUMO, respectively. μ_e is the electronic chemical potential. A and B subscripts stand for NO_x and $(WO_3)_n$, respectively.

Densities of states (DOS) were also calculated in order to analyze the band structures and Fermi level changes of WO_3 clusters, during the NO_x adsorption.

3. Results and Discussion

3.1. NO Adsorption on the $(WO_3)_n$ ($n = 2$–6) Clusters. Figure 1 demonstrates all optimized cyclic structures of WO_3. In order to evaluate their abilities for using as the gas sensors, cyclic WO_3 clusters have been analyzed through the quantum chemistry approach.

Since there are different adsorption sites on WO_3 clusters for NO adsorption, interfacial interactions between the clusters and NO molecule will be different from the energy point of view. The most important parameters which affect the adsorption energy are the adsorption site and NO conformation on the clusters. This means that for better analysis of the systems, it is necessary to investigate different orientations of NO molecule on the different sites of the clusters. These investigations have been illustrated in Figure 2. This figure only shows the most stable structures after optimization by X3LYP functional.

Theoretical calculations confirmed that NO adsorption through the N-head ($ON\cdots WO_3$) is the most stable orientations through which the most adsorption energy is obtained (Table 1).

Figure 3 shows the potential energy diagram for NO adsorption on W_2O_6 clusters as an example. According to Figure 3, relaxed NO molecule is close to WO_3 clusters from a distance of 6 Å. This figure shows the adsorption energy as a function of $N\cdots W$ distance.

Calculated adsorption energies of all studied systems have been reported in Table 1. Considering Table 1, it can be concluded that X3LYP functional predicts stronger physical adsorption than B3LYP. Correlation between the size of the cluster and adsorption energy is according to n: $2 > 3 \geq 4 > 5 > 6$ at the X3LYP functional. The energy of adsorption for the most stable structures of ON @ W_2O_6 and NO @ W_2O_6 complexes is 0.685 and 0.340 eV, respectively. Since ON @ W_2O_6 complex is a better candidate than others from the energy viewpoint, in the next stage of our study, we concentrated on this type of interaction and it has been fully investigated through the quantum chemistry approach.

Table 1: Energy of adsorption for all structures (in −eV) and adsorption through O-head (N-head) of NO.

Method	W_2O_6	W_3O_9	W_4O_{12}	W_5O_{15}	W_6O_{18}
B3LYP	0.147 (0.205)	0.221 (0.244)	0.202 (0.218)	0.107 (0.194)	0.180 (0.195)
X3LYP	0.340 (0.685)	0.230 (0.276)	0.230 (0.247)	0.212 (0.220)	0.209 (0.215)

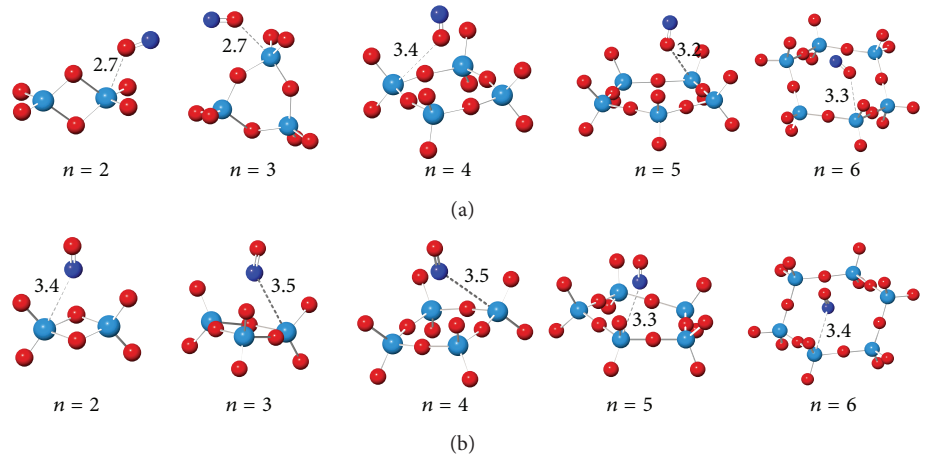

Figure 2: Optimized structures of NO adsorption on the $(WO_3)_n$ clusters at X3LYP functional: (a) through the O-head and (b) through the N-head of NO molecule.

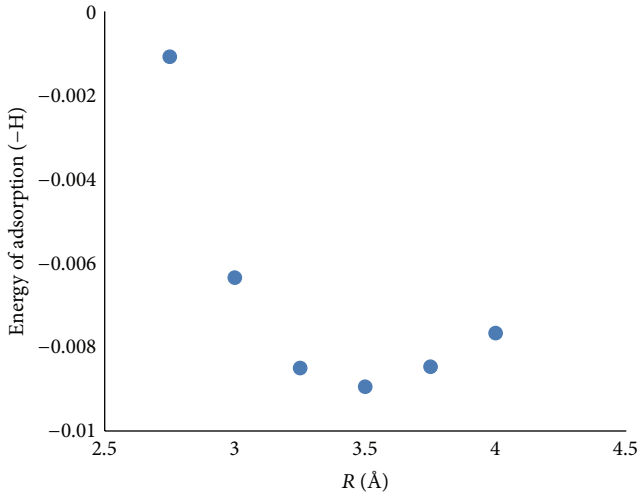

Figure 3: Potential energy diagram for NO-$(WO_3)_2$ system.

Table 2: Calculated quantum reactivity indices for NO adsorption.

System	η (eV)	ΔN
ON @ W_2O_6	7.318	0.019
ON @ W_3O_9	7.883	0.051
ON @ W_4O_{12}	8.190	0.059
ON @ W_5O_{15}	8.153	0.059
ON @ W_6O_{18}	8.145	0.063

Table 2 shows the quantum chemistry reactivity indices for the stable structures. According to Table 2, charge transfer and chemical hardness have been increased from NO to the surface with increase in the $(WO_3)_n$ clusters sizes. Higher values of the charge transfer and chemical hardness mean that increase in the size of the system makes its electronic charges unstable and lowers its flexibility.

Natural population analysis confirms that there are considerable orbital overlap between W and N atoms of the clusters and NO molecule, respectively. Natural charges for N and W atoms of NO @ W_2O_6 complex are +0.08, +1.5*e* before adsorption and +0.12, +1.38*e* after adsorption, respectively. This type of charge fluctuation indicates the charge flow from the adsorbate to the surface.

The influence of NO adsorption on the electronic properties of the tungsten oxide clusters was also investigated. DOS spectra of WO_3 and ON @ WO_3 structures have been compared. As an example, Figure 4 presents DOS spectra of W_2O_6 cluster before and after adsorption. Considering all systems, it was found that band gap (E_g) changes are between 4.37 and 9.91% after the adsorption process. These results show that the adsorption of NO molecule cannot significantly affect the E_g and conductivity of the nanostructures while the Fermi level energy (E_{FL}) is shifted by 0.385 eV towards the higher energies. Due to this effect, metal oxide work function (Φ) is decreased. Finally, the dispersion corrected functional, X3LYP, shows that the theoretical results which have been computed by this method differ from the B3LYP in all cases. This means that the inclusion of an empirical dispersion correction to the density functional amplifies the calculated energies of physisorption.

3.2. NO_2 Adsorption on the $(WO_3)_n$ (n = 2–6) at the X3LYP Functional. Since, in the previous section, stronger adsorptions were obtained by X3LYP functional, this method is chosen for analysis of NO_2 @ $(WO_3)_n$ systems. Four models

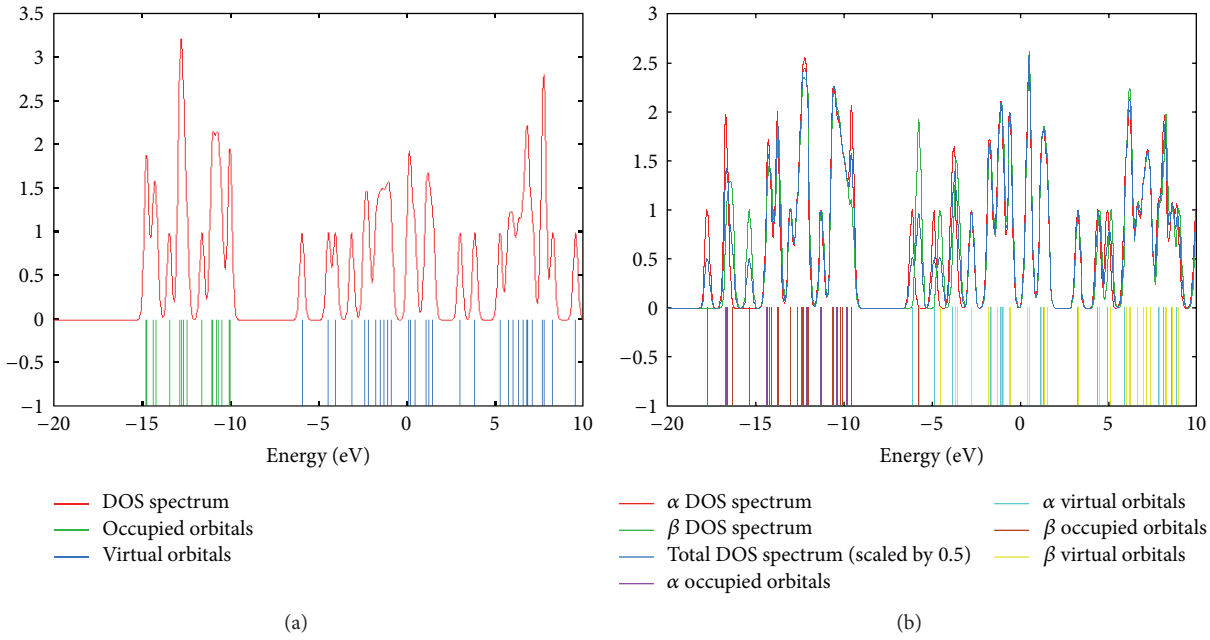

Figure 4: DOS spectra of W_2O_6 surfaces (a) before adsorption of NO and (b) after adsorption.

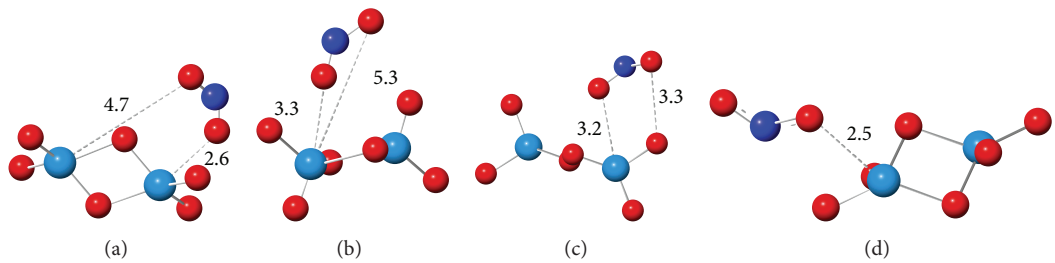

Figure 5: Different models of NO_2 adsorption on W_2O_6.

Table 3: Calculated energy of adsorption (in −eV) for NO_2 @ $(WO_3)_n$ complexes.

Model	$n = 2$	$n = 3$	$n = 4$	$n = 5$	$n = 6$
a	0.361	0.325	−0.961	0.194	0.250
b	0.192	0.172	0.158	0.124	0.109
c	0.193	0.175	0.161	0.127	0.116
d	2.003	0.631	0.489	0.362	0.292

Table 4: Calculated quantum chemistry reactivity indices for NO_2 adsorption.

System	ΔN	η (eV)
NO_2 @ W_2O_6	0.013	7.318
NO_2 @ W_3O_9	0.011	7.883
NO_2 @ W_4O_{12}	0.012	8.140
NO_2 @ W_5O_{15}	0.006	8.153
NO_2 @ W_6O_{18}	0.002	8.195

of adsorption have been considered. Figure 5 shows these adsorption models (a)–(d) for NO_2 @ W_2O_6 complex as an example.

Adsorption energies for NO_2 @ $(WO_3)_2$ systems have been calculated and reported in Table 3. According to Table 3, model d is the best configuration for NO_2 adsorption from the energy point of view, 2.0 eV. This extent of adsorption energy corresponds to NO_2 chemisorption on the W_2O_6 cluster. Considering all possible models, it is confirmed that the reactivity order is according to the following: d > a > c > b. Obtained correlation between the size of the cluster and adsorption energy is according to the following: $n = 2 > 3 > 4 > 5 > 6$.

Different behavior of NO_2 adsorption on $(WO_3)_n$ (n = 2–6) has been seen in the Fermi level shifting character. As an example, W_2O_6 band gap is decreased from 10.10 to 9.97 eV after adsorption. Due to NO_2 adsorption, Fermi level is shifted by 0.26 eV towards high-energy region (from −4.95 to −4.69 eV).

Charge transfer and chemical hardness changes during the NO_2 adsorption have been calculated and reported in Table 4.

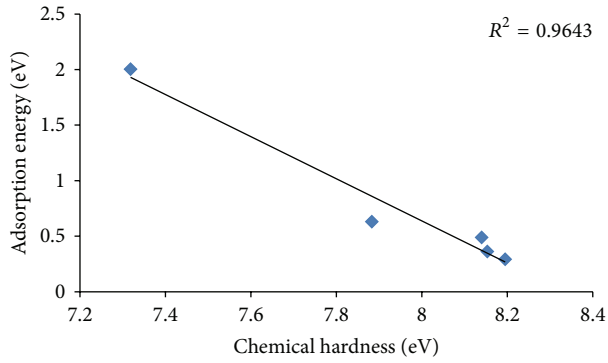

Figure 6: Linear correlation between the chemical hardness and adsorption energy.

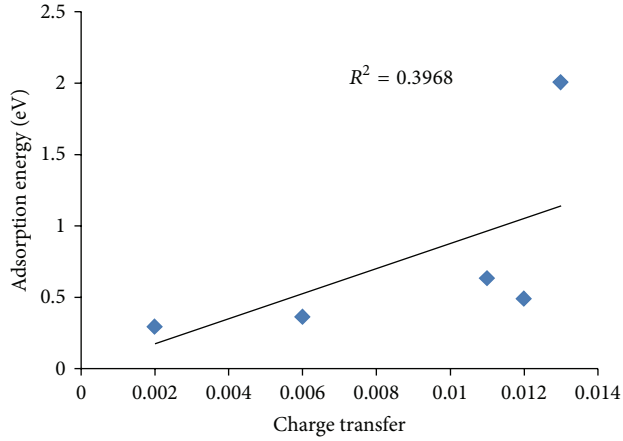

Figure 7: Weak linear correlation between the charge transfer parameter and adsorption energy.

According to Table 4, there is a similarity between NO_2 and NO adsorption behavior from the chemical hardness viewpoint. Considering the electronic charge transfer, different behavior was seen. This means that increase in the size of the cluster promotes the chemical hardness while reducing the charge transfer between NO_2 and clusters. Figures 6 and 7 show the obtained linear correlation of the adsorption energy-chemical hardness and adsorption energy-charge transfer, respectively. Good correlation between the adsorption energy and chemical hardness is obtained while this correlation is weak in the case of the charge transfer. Therefore, it can be concluded that the extent of chemical hardness fluctuation is one of the important parameters in sensing properties of the metal oxide clusters.

Natural population analysis confirms that W atom of W_2O_6 in the vicinity of NO_2 molecule has a positive character and carries a charge of +1.6e. One O atom of NO_2 molecule which is closer to W atom of the nanocluster has obtained more negative charge than the other. Due to this charge transfer from W, oxygen atomic charge is changed from −0.24 to −0.27e.

Comparing between the negative character of O atom and positive character of W atom, it can be concluded that W and O atoms do not exist as W^{6+} and O^{2-} as in the bulk of WO_3. Therefore, we can conclude that there are considerable orbital overlaps between W and O atoms. Back-donation of lone pair electrons of O atoms to the vacant d orbitals of W atoms is the source of this covalent character for W–O bonds in the case of chemical adsorption.

4. Conclusions

The adsorption of NO_x ($x = 1, 2$) molecules on the tungsten oxide clusters was investigated using density functional theory calculations by B3LYP and X3LYP functionals. During the adsorption of NO_x on the $(WO_3)_n$ ($n = 2$–6) nanoclusters, energy is released with a significant charge transfer from the NO_x to the nanoclusters. The results showed that the adsorption energy depends on the size of the cluster. X3LYP functional predicts stronger adsorption than B3LYP. W_2O_6 cluster is the best candidate for NO_x adsorption from the energy point of view. In order to have a meaningful understanding of molecular changes during the adsorption process, quantum chemistry reactivity indices such as chemical hardness and charge transfer parameters were evaluated. Obtained results from the natural bond orbital and electronic density of states analysis confirmed the electronic charge transfer from the adsorbates to the WO_3 clusters and Fermi level shifting after adsorption, respectively.

Conflict of Interests

The authors declare that there is no conflict of interests regarding the publication of this paper.

Acknowledgment

Research council of Ferdowsi University of Mashhad is acknowledged for financial supports (Grants nos. 3/18880 and 1390/07/25).

References

[1] S. M. Kanan, O. M. El-Kadri, I. A. Abu-Yousef, and M. C. Kanan, "Semiconducting metal oxide based sensors for selective gas pollutant detection," *Sensors*, vol. 9, no. 10, pp. 8158–8196, 2009.

[2] G. Korotcenkov, I. Blinov, M. Ivanov, and J. R. Stetter, "Ozone sensors on the base of SnO_2 films deposited by spray pyrolysis," *Sensors and Actuators B: Chemical*, vol. 120, no. 2, pp. 679–686, 2007.

[3] B. Timmer, W. Olthuis, and A. van den Berg, "Ammonia sensors and their applications—a review," *Sensors and Actuators, B: Chemical*, vol. 107, no. 2, pp. 666–677, 2005.

[4] M. Stankova, X. Vilanova, J. Calderer et al., "Sensitivity and selectivity improvement of rf sputtered WO_3 microhotplate gas sensors," *Sensors and Actuators B: Chemical*, vol. 113, no. 1, pp. 241–248, 2006.

[5] Z. Liu, T. Yamazaki, Y. Shen, T. Kikuta, and N. Nakatani, "Influence of annealing on microstructure and NO_2-sensing properties of sputtered WO_3 thin films," *Sensors and Actuators, B: Chemical*, vol. 128, no. 1, pp. 173–178, 2007.

[6] G. Korotcenkov, "Metal oxides for solid-state gas sensors: what determines our choice?" *Materials Science and Engineering B: Advanced Functional Solid-State Materials*, vol. 139, no. 1, pp. 1–23, 2007.

[7] I. N. Yakkovin and M. Gutowski, "Driving force for the WO_3(001) surface relaxation," *Surface Science*, vol. 601, no. 6, pp. 1481–1488, 2007.

[8] M. B. Klepser and B. M. Bartlett, "Anchoring a molecular iron catalyst to solar-responsive WO_3 improves the rate and selectivity of photoelectrochemical water oxidation," *Journal of the American Chemical Society*, vol. 136, no. 5, pp. 1694–1697, 2014.

[9] C. Lemire, D. Lollman, A. Mohammad, E. Gillet, and K. Aguir, "Reactive R.F. magnetron sputtering deposition of WO_3 thin films," *Sensors and Actuators B*, vol. 84, pp. 43–48, 2002.

[10] E. Comini, M. Ferroni, V. Guidi, G. Faglia, G. Martinelli, and G. Sberveglieri, "Nanostructured mixed oxides compounds for gas sensing applications," *Sensors and Actuators B: Chemical*, vol. 84, no. 1, pp. 26–32, 2002.

[11] H. Xia, Y. Wang, F. Kong et al., "Au-doped WO_3-based sensor for NO_2 detection at low operating temperature," *Sensors and Actuators B: Chemical*, vol. 134, no. 1, pp. 133–139, 2008.

[12] D. Filippini, L. Fraigi, R. Aragón, and U. Weimar, "Thick film Au-gate field-effect devices sensitive to NO_2," *Sensors and Actuators, B: Chemical*, vol. 81, no. 2-3, pp. 296–300, 2002.

[13] J. Yang and P. K. Dutta, "Promoting selectivity and sensitivity for a high temperature YSZ-based electrochemical total NO_x sensor by using a Pt-loaded zeolite Y filter," *Sensors and Actuators B: Chemical*, vol. 125, no. 1, pp. 30–39, 2007.

[14] V. Khatkoa, S. Vallejosa, J. Caldererb et al., "Micro-machined WO_3-based sensors with improved characteristics," *Sensors and Actuators B: Chemical*, vol. 140, no. 2, pp. 356–362, 2009.

[15] M. Penza, M. A. Tagliente, L. Mirenghi, C. Gerardi, C. Martucci, and G. Cassano, "Tungsten trioxide (WO_3) sputtered thin films for a NO_x gas sensor," *Sensors and Actuators B: Chemical*, vol. 50, no. 1, pp. 9–18, 1998.

[16] R. Boulmani, M. Bendahan, C. Lambert-Mauriat, M. Gillet, and K. Aguir, "Correlation between rf-sputtering parameters and WO_3 sensor response towards ozone," *Sensors and Actuators B: Chemical*, vol. 125, no. 2, pp. 622–627, 2007.

[17] J. Guérin, M. Bendahan, and K. Aguir, "A dynamic response model for the WO_3-based ozone sensors," *Sensors and Actuators B: Chemical*, vol. 128, no. 2, pp. 462–467, 2008.

[18] B. Cole, B. Marsen, E. Miller et al., "Evaluation of nitrogen doping of tungsten oxide for photoelectrochemical water splitting," *The Journal of Physical Chemistry C*, vol. 112, no. 13, pp. 5213–5220, 2008.

[19] R. R. Kharade, S. R. Mane, R. M. Mane, P. S. Patil, and P. N. Bhosale, "Synthesis and characterization of chemically grown electrochromic tungsten oxide," *Journal of Sol-Gel Science and Technology*, vol. 56, no. 2, pp. 177–183, 2010.

[20] F. Wang, C. Di Valentin, and G. Pacchioni, "Electronic and structural properties of WO_3: a systematic hybrid DFT study," *Journal of Physical Chemistry C*, vol. 115, no. 16, pp. 8345–8353, 2011.

[21] J. Kong, N. R. Franklin, C. Zhou et al., "Nanotube molecular wires as chemical sensors," *Science*, vol. 287, no. 5453, pp. 622–625, 2000.

[22] D. W. Rothgeb, E. Hossain, A. T. Kuo, J. L. Troyer, and C. C. Jarrold, "Structures of anion and neutral clusters determined by anion photoelectron spectroscopy and density functional theory calculations," *The Journal of Chemical Physics*, vol. 131, Article ID 044310, 2009.

[23] N. J. Mayhall, D. W. Rothgeb, E. Hossain, K. Raghavchair, and C. C. Jarrold, "Electronic structures of $MoWO_y^-$ and $MoWO_y$ determined by anion photoelectron spectroscopy and DFT calculations," *The Journal of Chemical Physics*, vol. 130, p. 124313, 2009.

[24] M. J. Frisch, G. W. Trucks, H. B. Schlegel et al., *Gaussian 09, Revision D.01*, Gaussian, Inc., Wallingford, Conn, USA, 2009.

[25] T. H. Dunning and P. J. Hay, *Modern Theoretical Chemistry*, vol. 3, Plenum Press, New York, NY, USA, 1977, edited by H. F. Schaefer III.

[26] R. Ditchfield, W. J. Hehre, and J. A. Pople, "Self–consistent molecular–orbital methods. IX. An extended Gaussian–type basis for molecular–orbital studies of organic molecules," *The Journal of Chemical Physics*, vol. 54, no. 2, p. 724, 1971.

[27] K. D. Dobbs and W. J. Hehre, "Molecular orbital theory of the properties of inorganic and organometallic compounds 5. Extended basis sets for first-row transition metals," *Journal of Computational Chemistry*, vol. 8, no. 6, pp. 861–879, 1987.

[28] A. E. Reed, L. A. Curtiss, and F. Weinhold, "Intermolecular interactions from a natural bond orbital, donor-acceptor viewpoint," *Chemical Reviews*, vol. 88, no. 6, pp. 899–926, 1988.

[29] A. E. Reed, R. B. Weinstock, and F. Weinhold, "Natural population analysis," *The Journal of Chemical Physics*, vol. 83, no. 2, pp. 735–746, 1985.

[30] T. Koopmans, "Ordering of wave functions and eigenenergies to the individual electrons of an atom," *Physica*, vol. 1, pp. 104–113, 1933.

[31] W. Kohn and L. J. Sham, "Self-consistent equations including exchange and correlation effects," *Physical Review Letters*, vol. 140, pp. A1133–A1138, 1965.